MOLECULAR PHARMACOLOGY, 22:304–309

Cholinergic Muscarinic Receptor in Synaptosomal Membranes

Heterogeneity of Binding Sites for L-[^{3}H]Quinuclidinyl Benzilate

JOSÉ S. AGUILAR,[1] PEDRO J. I. SALAS, AND EDUARDO DE ROBERTIS

Instituto de Biología Celular, Facultad de Medicina, Universidad de Buenos Aires, Buenos Aires (1121), Argentina

Received August 24, 1981; Accepted April 21, 1982

SUMMARY

We studied the binding of radioactive L-quinuclidinyl benzilate (L-[^{3}H]QNB) to muscarinic cholinergic receptor sites of synaptosomal membranes of cat cerebral cortex. The experimental data were analyzed with the use of the Fortran IV program NLIN2, in an IBM/360 computer system DOS. The data obtained were compared with the model for n number of heterogeneous sites (n = 1, 2, or 3), and also with a model for cooperative bivalent sites. The best fitting was obtained with the two-population site model (K_{D_1} = 5.2 and K_{D_2} = 144 pM; B_{max_1} = 366 and B_{max_2} = 558 pmoles/g of protein) when the data were analyzed by the Scatchard equation ($p < 0.01$ according to Fischer's F-test). Competition with the muscarinic antagonist atropine and scopolamine gave IC_{50} values, respectively, of 1.4 and 3.4, and Hill coefficients of about 1. Competition with the muscarinic agonist oxotremorine and with carbamylcholine gave IC_{50} values, respectively, of 0.9 and 47 μM, and the Hill coefficients were 0.70 and 0.56. Consistent with the heterogeneity of sites found by equilibrium binding, heterogeneity was also observed in experiments of kinetic binding. The dissociation was biphasic, with a rapid component having $k_{-2} = 37.7 \times 10^{-3}$ min^{-1}, and a slow component having $k_{-1} = 4.8 \times 10^{-3}$ min^{-1}. The two-site model gave a much better fitting of the dissociation data than did the one-site model ($p < 0.01$, F-test). Because of the equilibrium and dissociation results, the association data were analyzed by the two-site model. A fast association component ($k_{+1} = 4.9 \times 10^{-4}$ pmoles^{-1} min^{-1}) and a slow association component ($k_{+2} = 1.1 \times 10^{-4}$ pmoles^{-1} min^{-1}) were found. The constants calculated from kinetic data for the two-site model were K_{D_1} = 9.7 pM and K_{D_2} = 342 pM, which showed little difference with those obtained by equilibrium binding. The results suggest the existence of two independent site populations for L-[^{3}H]QNB binding in synaptosomal membranes of the cat cerebral cortex.

INTRODUCTION

[^{3}H]QNB[2] has been used extensively to label muscarinic receptors (cf. refs. 1 and 2). The most widely used binding assay (3) consists of the simultaneous determination of total binding and of nonspecific binding, in the presence of a suitable inhibitor, at a concentration that labels all receptor sites. The difference between the two determinations represents the true specific binding to the muscarinic receptor. By using this technique on synaptosomal membranes of cat cerebral cortex (4), we detected a single set of saturable sites for [^{3}H]QNB with a K_D of 0.34 nM and a B_{max} of 2.2 nmoles/g of protein. Single-site binding has been generally reported in the literature, not only for central but also for cardiac and other peripheral muscarinic receptors. Fields *et al.* (5) observed that the K_D value was inversely related to the concentration of receptor in the assay, the limiting factor in this case being the specific radioactivity of the ligand (6). They found that, with the highly labeled QNB available, determinations of K_D could be carried out at concentrations of receptor as low as 2 pM (5).

The recent introduction of the L-isomer of [^{3}H]QNB, instead of the previously used racemic ligand, facilitated the assay even more, since one could expect some competition for binding from the D-isomer (7). In the present work, we took advantage of this stereospecific ligand to repeat our previous experiments on the synaptosomal membranes of cat cerebral cortex, and we were able to reduce considerably the amount of receptor required for the assay. This new investigation has resulted in the recognition of the possible existence of two saturable sites for L-[^{3}H]QNB, both of which have K_D values lower than the one previously reported (4).

MATERIALS AND METHODS

Membrane preparation. To isolate a crude synaptosomal membrane fraction, the gray matter of the cerebral

This work was supported by grants from CONICET and SECYT of Argentina.

[1] Fellow of the Lectoure Foundation.

[2] The abbreviation used is: QNB, quinuclidinyl benzilate.

0026-895X/82/050304-06$02.00/0

cortex of cat brain was dissected in the cold and rapidly homogenized to 10% in 0.32 M sucrose. The crude mitochondrial fraction, obtained as described in ref. 8, was subjected to osmotic shock in distilled water, followed by centrifugation at 20,000 × *g* for 30 min. The sediment (i.e., the M_1 fraction) obtained, which contained myelin, mitochondria, and synaptosomal membranes, was kept frozen at −60° until used for binding. Before the assay, the membranes were washed twice with buffer and centrifuged to eliminate any possible soluble endogenous inhibitor. Similar binding values were obtained with fresh membranes and with those frozen and thawed once.

Binding assays. For each binding assay, aliquots of membranes containing 40 μg of protein, as determined by the method of Lowry *et al.* (9), were resuspended in 4 ml of 50 mM PO_4 ($Na^+ - K^+$) buffer (pH 7.4). Incubation for the binding was carried out for 50 min at 37° in a Dubnoff apparatus, under constant shaking.

Binding experiments conducted between 10 and 60 min of incubation and with the minimal concentration of ligand used (i.e., 6 pM L-[^{3}H]QNB) showed that complete equilibrium had been reached at 40 min. At the end of the incubation period, the samples (incubated in triplicate or quadruplicate) were filtered through GF/B glass filters (Whatman), and washed three times with 5 ml of buffer. The filters were dried at 60° for 1 hr; 10 ml of Bray's (19) scintillation solution were then added and the samples were counted in a Tracor analytical scintillation spectrometer. To determine nonspecific binding, parallel experiments were carried out in the presence of 5 μM atropine. In all cases, specific binding represented more than 90% of the total.

Kinetic assays. Kinetic studies were carried out using the same filtration assay. For the association, 50 ml of suspension containing 10 μg of protein per milliliter were used. To these membranes, maintained under stirring at 37°, 50 pM or 500 pM L-[^{3}H]QNB was added and rapidly mixed. At different time intervals, 4-ml samples were removed and filtered as indicated above. Parallel experiments were carried out to assay for nonspecific binding. The dissociation assay was performed in a similar way on membranes that had reached equilibrium binding with 50 pM or 400 pM L-[^{3}H]QNB. At zero time, atropine was added to the suspension to reach a 5 μM concentration and, at timed intervals, 4-ml samples were filtered. Nonspecific binding was also assayed by carrying the equilibrium binding in the presence of atropine.

L-[^{3}H]QNB (Lot 1231-181) was purchased from New England Nuclear Corporation (Boston, Mass.), and the specific radioactivity was 40.2 Ci/mmole.

Data analysis. The specific binding data, a total of 55 experimental points from 7 experiments carried out in quadruplicate, were fed into the computer and analyzed by a nonlinear regression program using the least-squares estimation of parameters (11). The Fortran IV program used is described as NLIN2 in the IBM Share Library Distribution 3094. The calculations were made with the use of an IBM/360 computer system DOS. The experimental data were compared with the following models.

1. A model describing the binding of homogeneous ligands to heterogeneous sites without cooperativity (12). This model is given by the following equation:

$$B = \sum_{i=1}^{n} B_{\max_i} \frac{F}{K_{D_i} + F} \tag{1}$$

where B is the total amount of specifically bound ligand; n is the number of populations of binding sites; F is the free ligand concentration, calculated as F = total concentration − total bound; and $B_{\max_i}$ is the total number of binding sites of the ith population. Equation 1 was applied to cases in which n was 1, 2, or 3.

The equilibrium binding data were also analyzed according to the Scatchard equation for one-site populations:

$$\frac{B}{F} = \frac{B_{\max}}{K_D} - \frac{B}{K_D} \tag{2}$$

and for two-site populations (see ref. 13):

$$\frac{B}{F} = \frac{\begin{aligned} &K_{A_1}(B_{\max_1} - B) + K_{A_2}(B_{\max_2} - B) \\ &+ \{[K_{A_1}(B_{\max_1} - B) + K_{A_2}(B_{\max_2} - B)]^2 \\ &- 4K_{A_1}K_{A_2}B[B - (B_{\max_1} + B_{\max_2})]\}^{1/2} \end{aligned}}{2} \tag{3}$$

Notice that in Eq. 3, $K_{A_i} = K_{D_i}^{-1}$.

2. A model describing the binding of homogeneous ligands to homogeneous cooperative bivalent sites (13). This model is given by the following equation:

$$B = \frac{FB_{\max}K_A(1 + \beta K_A F)}{1 + 2K_A F + \beta K^2{}_A F^2} \tag{4}$$

where K_A is the association constant and β is the cooperativity coefficient. In Eq. 4, $\beta = 1$ implies no cooperativity, $\beta > 1$ implies positive cooperativity, and $\beta < 1$ implies negative cooperativity. These models are valid only under equilibrium conditions of binding.

The kinetic data were also analyzed by the nonlinear regression program using the following equations for one or two independent sites, and the additive properties of the binding. For association:

$$B_t = \sum_{i=1}^{n} B_{\text{eq}_i}(1 - \exp(-k_{\text{obs}_i}t)) \tag{5}$$

The association constant k_{+1_i} (14) was calculated from the expression of k_{obs_i}:

$$k_{\text{obs}_i} = k_{+1_i}F + k_{-1_i} \tag{6}$$

For dissociation:

$$B_t = \sum_{i=1}^{n} B_{\text{eq}_i}\exp(-k_{-1_i}t) \tag{7}$$

where B_t is specific binding at time t, B_{eq_i} is specific binding at equilibrium, and k_{-1_i} is the dissociation constant of the ith site.

The fitting of the experimental data to each model is measured in terms of $\sum_j (\hat{Y}_j - Y_j)^2$, where $\hat{Y}_j$ is the theoretical value and Y_j is the experimental value for the jth experimental point (Table 1).

The statistical significance was tested by Fischer's F-test (15) for the null hypothesis—$H_0: \sum_j (\hat{Y}_j - Y_j)^2$ (for a model Y) $= \sum_j (\hat{X}_j - X_j)^2$ (for a model X)—versus the alternative hypothesis—$H_1: \sum_j (\hat{Y}_j - Y_j)^2 > \sum_j (\hat{X}_j - X_j)^2$. The probabilities of H_0 were expressed as $p < \cdots$.

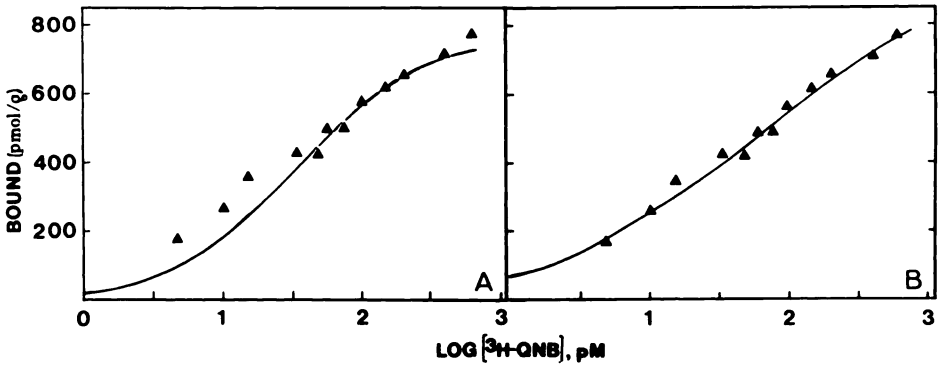

FIG. 1. *Specific L-[^{3}H]QNB binding curve for synaptosomal membranes from cat brain: log concentration plot*

A, binding data are superimposed on a theoretical curve obtained by computer for one mass-action site; B, the same binding data, but on a theoretical curve for two independent sites. Binding was carried out as described under Materials and Methods. Data represent the means of seven experiments carried out in quadruplicate and analyzed by a nonlinear regression program using the least-squares estimation of parameters (14). Each point represents the average of at least four independent measurements with a standard deviation lower than 15% except for the first *left* point, where the standard deviation was about 30%.

RESULTS

Figure 1 shows the experimental data for L-[^{3}H]QNB binding in the range 6–600 pM. Saturation is reached at a concentration of about 200 pM. In Table 1, the binding parameters were analyzed by the heterogeneous-site model without cooperativity (Eq. 1) and by the homogeneous cooperative bivalent-site model (Eq. 2). Using Fischer's *F*-test there is no statistical difference among the two-site, three-site, and cooperative models. However, there is a slight improvement of the fitting when the two-site model is compared with the one-site model ($p < 0.2$; $df = 53$ and 51). In Fig. 1 the experimental data (the means for each concentration) are superimposed on the theoretical curves for the single-site model and the two independent-site models. Visually, the fitting appears to be more accurate for the second model. This conclusion is better borne out when the results are plotted according to the Scatchard equation (Eqs. 2 and 3) (Fig. 2A) describing a curvilinear plot. In Fig. 2A the straight lines correspond to the theoretical two-site model, obtained by computer analysis of Eq. 1. In Fig. 2B all experimental data are included in the same type of plot. The least-squares regression analysis was performed for the one-site model (Eq. 2) and the two-site model (Eq. 3). In the first case a K_D value of 33 pM and B_{max} value of 875 pmoles/g of protein were obtained. The two-site model gave the same values for the binding parameters shown in Table 1. In this case the variance analysis by the *F*-test showed a very significant improvement ($p < 0.01$; $df = 53$ and 51) for the two-site model. These results may be due to a higher sensitivity of the Scatchard analysis in detecting heterogeneity of sites. The homogeneous cooperative-site model also provides a good fitting with $\beta = 0.14$. The model for three populations of sites gives a K_{D_3} value of 4.6×10^6 M and a B_{max_3} value of 10^6 μmoles/g of protein; these values are too high and have no real meaning. For these reasons the two populations and the cooperative models appear to be the most appropriate for fitting the experimental data.

In Table 1 the values for K_D and B_{max} of the other models are also shown. In Fig. 3 the binding data are plotted according to the Hill equation. A Hill coefficient of 0.69 was obtained, which agrees with a possible negative cooperativity, or a multiple-site model.

To analyze the specificity of L-[^{3}H]QNB binding for the muscarinic receptor, competition experiments were carried out with the antagonists atropine and scopolamine, and with the agonists oxotremorine and carbamylcholine (Fig. 4). Binding was assessed with 50 pM L-[^{3}H]QNB in the presence of increasing concentrations of inhibitor. For the two antagonists the displacement obtained was in the nanomolar range, whereas for the agonists it was in the micromolar range (Table 2). These values are similar to those previously found using the racemic [^{3}H]QNB (3, 5). The Hill numbers for the antagonists were close to unity. For the agonists, the values of N_H were below 1, suggesting different populations of binding sites for these ligands (Table 2).

To better analyze the possible existence of heterogeneous binding sites, we carried out kinetic studies in experiments of association-dissociation binding. For the association, the time course was analyzed between 1 and 120 min at 37°. After 90 min, there was a certain loss of

TABLE 1

Binding parameters obtained by equilibrium and analyzed by the one-, two-, and three-site models, and by the cooperativity model, as described under Materials and Methods (Eqs. 1 and 4)

For the meaning of $\Sigma_j (\hat{Y}_j - Y_j)^2$, see text. In the cooperativity model, $K_{D_1} = 1/K_A$. K_D values are expressed as picomolar and B_{max} as picomoles per gram of protein.

Model	K_{D_1}	K_{D_2}	K_{D_3}	B_{max_1}	B_{max_2}	B_{max_3}	β	$\Sigma_j (\hat{Y}_j - Y_j)^2$
One population	34.2	—	—	767.1	—	—	1	4.34×10^5
Two populations	5.2	144		336.0	558.2	—	1	3.68×10^5
Three populations	2.2	49.4	4.6×10^6	205.8	475.3	10^6	1	3.63×10^5
Cooperativity	20.4	—	—	923.0	—	—	0.14	3.71×10^5

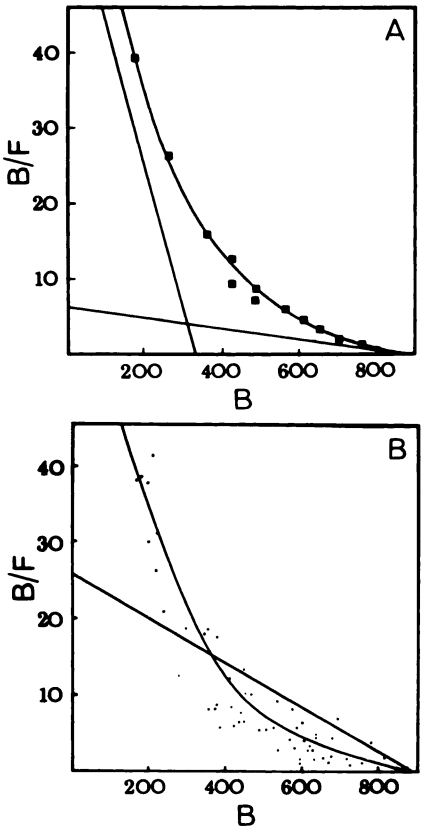

FIG. 2. *L-[^{3}H]QNB binding curve as in Fig. 1, but plotted according to the Scatchard equation*

A. The means of the data are fitted on a curve. The *straight lines* represent the two individual binding components obtained by computer analysis. The higher-affinity site had a K_{D_1} of 5.2 pM and a B_{max_1} of 336 pmoles/g of protein. The second site had a K_{D_2} of 144 pM and a B_{max_2} of 538.2 pmoles/g of protein.

B. All of the experimental data are fitted. The curve represents the least-squares regression for Eq. 3 and the *straight line* represents the least-squares regression for Eq. 2. The first regression is significantly better than the second one ($p < 0.01$).

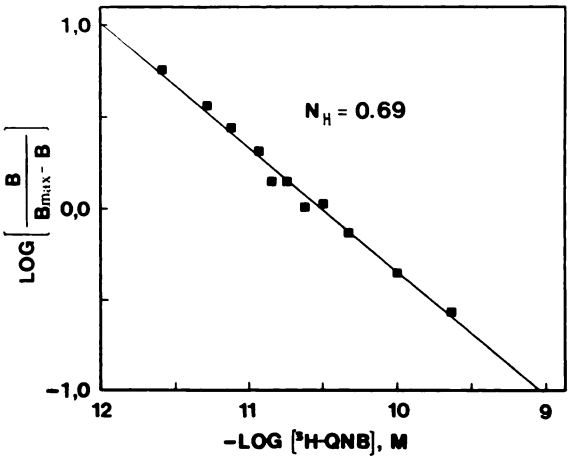

FIG. 3. *Specific L-[^{3}H]QNB binding curve as in Fig. 1, but plotted according to the Hill equation*

The line was obtained by linear regression analysis of data ($r = 0.99$); the B_{max} was the sum of the B_{max} of the two affinity sites obtained through Eqs. 1 and 3.

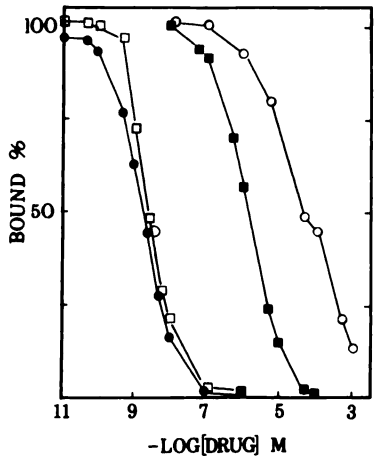

FIG. 4. *Inhibition of the specific L-[^{3}H]QNB binding from synaptosomal membranes by muscarinic agents*

Binding assays were carried as described under Materials and Methods with 50 pM L-[^{3}H]QNB. Each point represents the mean of quintuplicates. ○——○, Carbamylcholine, 100% = 3452 ± 106 dpm (n = 4); ■——■, oxotremorine, 100% = 2242 ± 141 dpm (n = 4); □——□, scopolamine, 100% = 2050 dpm (n = 1); ●——●, atropine, 100% = 5890 dpm (n = 1).

binding, probably due to denaturation of the receptor. In Fig. 5A, only the values obtained between 1 and 40 are represented. The fitting was obtained by using Eq. 5. In Fig. 5A both the linear and the nonlinear theoretical curves are represented. In these association experiments, the equilibrium is reached at 40 min with 50 pM L-[^{3}H]QNB, and in less than 10 min with 400 pM L-[^{3}H]QNB. The association constants obtained using Eq. 4 were k_{+1}, 4.9 × 10^{-4} pM^{-1} min^{-1}; k_{+2}, 1.1 × 10^{-4} pM^{-1} min^{-1} (Table 3). When the one- and two-site models were analyzed by Fischer's F-test no significant differences were observed.

The kinetics of dissociation was studied between 1 and 60 min at 37°, after the binding with 50 or 400 pM L-[^{3}H]QNB had reached equilibrium. At zero time, atropine was added under stirring, to reach a final concentration of 5 μM. In Fig. 5B it is observed that the displacement of L-[^{3}H]QNB follows a biphasic curve, with a fast and a slow component, the last one reaching 50% of displacement at 60 min. For the rapid dissociation the k_{-2} value was 37.7 × 10^{-3} min^{-1}, and for the slow component the k_{-1} value was 4.8 × 10^{-3} min^{-1}. These values

TABLE 2

Relative potency of antagonists and agonists inhibiting L-[^{3}H]QNB specific binding to synaptosomal membranes

The IC_{50} values were obtained from the displacement curves shown in Fig. 4. The Hill coefficients (N_H) were calculated from logit-log plots. Observe that the IC_{50} values are in the nanomolar range for antagonists and in the micromolar range for agonists. The results are the means ± standard error of the mean of four experiments carried out in quintuplicate.

Drug	IC_{50}	N_H
Atropine	1.4 ± 0.4 nM	0.94 ± 0.08
Scopolamine	3.4 ± 1.0 nM	1.02 ± 0.07
Oxotremorine	0.9 ± 0.3 μM	0.70 ± 0.10
Carbamylcholine	47.0 ± 6.0 μM	0.56 ± 0.01

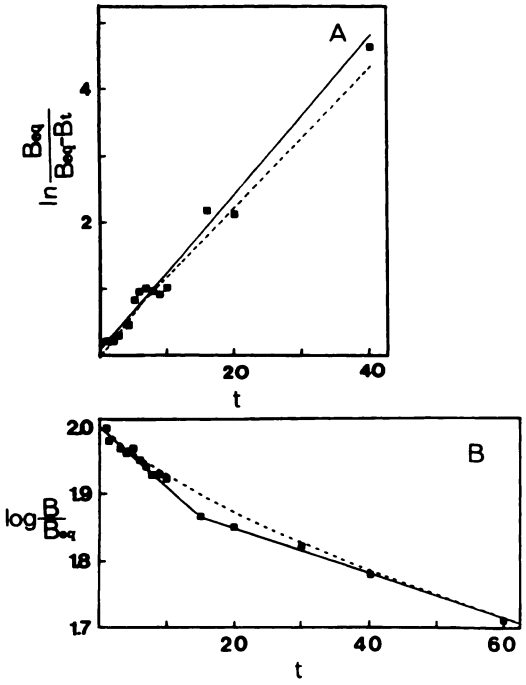

FIG. 5. *Kinetics of specific* L-*[^{3}H]QNB binding*

A. Association rate. Binding was carried out as described under Materials and Methods, using 50 pM L-[^{3}H]QNB. Following incubation at 37° for the times indicated, 4-ml samples of membranes (10 μg of protein per milliliter) were filtered through GF/B Whatman filters and then washed three times with 5 ml of cold incubation buffer. Each point represents the mean of two experiments carried out in triplicate. The *solid line* represents the single-site model; the *dashed line*, the two-site model.

B. Dissociation rate. Following equilibration for at least 10 min with 400 pM L-[^{3}H]QNB for 50 min at 37°, atropine was added to reach a 5 μM concentration. At the times indicated, 4-ml samples were filtered and washed as described above. Each point represents the mean of three experiments. (The plot for 50 pM L-[^{3}H]QNB is similar). *Solid lines* were drawn by eye; the *dashed line* represents the two-site model, which gives a much better fitting than the one-site model.

were calculated from Eq. 5. In this case there is a very significant improvement of the fitting using the two-site model ($p < 0.01$).

From these kinetic studies it is possible to calculate a K_{D_1} value of 9.7 pM for the slow dissociation component, and a K_{D_2} value of 342 pM for the fast component. As shown in Table 3, there is a good correlation between the K_D obtained by equilibrium binding and by kinetic studies (Table 3).

DISCUSSION

In most cases reported in the literature, cholinergic muscarinic receptors do not show heterogeneity of binding sites for antagonists. Equilibrium binding reveals a single mass-action kinetics with a Hill coefficient of 1, corresponding to a single class of sites without cooperativity. However, a few exceptions to this rule were observed. Using [^{3}H]scopolamine in neuroblastoma cells, a heterogeneity of binding sites was observed (16). Hammer *et al.* (17), using the antimuscarinic drug pirenzepine, could differentiate subclasses of muscarinic sites not detected by classic antagonists. Fisher *et al.* (18, 19) synthesized a number of muscarinic antagonists derived from quinuclidine which showed a certain pharmacological selectivity for different classes of muscarinic receptors; however, binding data were not reported.

Recently Ehlert *et al.* (20) reported two binding sites for L-[^{3}H]QNB with values for K_{D_1} of 30 pM and K_{D_2} of 640 pM in striatal membranes. These data were obtained by equilibrium binding.

Agonists behave differently from antagonists and cause displacement curves with Hill coefficients between 0.3 and 1.0; these could be explained in terms of negative cooperativity, desensitization, or multisite binding. Indeed, by the use of labeled agonists, it has been found that there are at least two independent subtypes of muscarinic receptors in brain (21, 22).

In the present investigation, using the L-isomer of [^{3}H]QNB, it has been possible to obtain evidence for the presence of two independent high-affinity binding sites for the muscarinic receptor in synaptosomal membranes of the cat cerebral cortex. The computer analysis of the equilibrium binding data by a nonlinear regression program showed a sightly better fitting for two independent-site models with Eq. 1 (Fig. 1). When the data were analyzed by the Scatchard equation, a significant statistical improvement of the fitting ($p < 0.01$) was obtained for the two-site model (Fig. 2). From both Eqs. 1 and 3, the two-site model permitted calculation of a K_{D_1} of 5.2 pM with a B_{max_1} of 336 pmoles/g of protein for the higher affinity site and a K_{D_2} of 144 pM with a B_{max_2} of 538.2 pmoles/g of protein for the second site. Also in support of this interpretation is the finding of a Hill coefficient of 0.69 for the experimental data (Fig. 3), which suggests either heterogeneity or negative cooperativity in the binding.

To investigate further the possible heterogeneity of central muscarinic receptors we carried out kinetic experiments of association and dissociation. The associa-

TABLE 3

Summary of data obtained by equilibrium and kinetics in the binding of L-*[^{3}H]QNB to synaptosomal membranes*

For definitions of constants see Eqs. 1–5.

	Site 1: high-affinity	Site 2: low-affinity
Equilibrium dissociation constants	K_{D_1} = 5.2 pM	K_{D_2} = 144 pM
Dissociation rate constants	$k_{-1} = 4.8 \times 10^{-3}$ min^{-1}	$k_{-2} = 37.7 \times 10^{-3}$ min^{-1}
Association rate constants	K_{obs_1} = 0.2 min^{-1}	K_{obs_2} = 0.08 min^{-1}
	$k_{+1} = 4.9 \times 10^{-4}$ pmole^{-1} min^{-1}	$k_{+2} = 1.1 \times 10^{-4}$ pmole^{-1} min^{-1}
Kinetic dissociation constants $K_{D_1} = k_{-1}/k_{+1}$	K_{D_1} = 9.7 pM	K_{D_2} = 342 pM
Kinetic K_D/equilibrium K_D	1.8	2.3

tion data could be fitted by either the one- or two-site model. The two-site model values obtained were as follows: $k_{+1} = 4.9 \times 10^{-4}$ pM^{-1} min^{-1}; $k_{+2} = 1.1 \times 10^{-4}$ pM^{-1} min^{-1}. Although in this case there are no statistical differences between the fittings for the one- and two-site models, the use of the second one is justified by the equilibrium and dissociation results.

The study of the dissociation of L-[^{3}H]QNB binding by atropine revealed a fast and a slow component. In this case the two-site model fitting was significantly better than the one-site ($p < 0.01$). The kinetic curve obtained is concave up, which, according to De Lean and Rodbard (23), does not agree with a negatively cooperative model.

The experiments in which L-[^{3}H]QNB was displaced with the antagonists atropine and scopolamine showed a Hill coefficient of 1, which suggests a single class of antagonist binding sites without cooperativity (Fig. 4). These results are in apparent contradiction with the heterogeneity of sites suggested by the data on equilibrium binding and dissociation kinetics for L-[^{3}H]QNB. These negative findings are difficult to explain. One possibility could be that displacement by antagonists is not a sensitive enough method with which to detect differences of affinity in the picomolar range. Another possibility is that with the antagonists the Hill coefficient is shifted near 1 because both ligands (i.e., QNB and atropine or scopolamine) have similar heterogeneous types of binding in the nanomolar range. We mentioned above that with [^{3}H]scopolamine (which has a lower affinity than L-[^{3}H]QNB), in neuroblastoma cells, it was possible to differentiate two K_D values in the nanomolar range (16). In this particular case it is evident that there are two populations of sites for this antagonist.

The results presented here suggest that, by the use of the L-isomer of [^{3}H]QNB and a smaller amount of receptor in the assay, it is possible to detect two binding sites in synaptosomal membranes of cat cerebral cortex with K_D values that are considerably lower than the single K_D value previously reported (4). This inverse relationship between receptor concentration and K_D had previously

REFERENCES

1. Birdsall, N. J. M., and E. G. Hulme. Biochemical studies on muscarinic acetylcholine receptors. *J. Neurochem.* **27**:7–16 (1976).
2. Birdsall, N. J. M., C. P. Berrie, A. S. V. Burgen, and E. C. Hulme. Modulation of the binding properties of muscarinic receptors, in *Receptors for Neurotransmitters and Peptide Hormones* (G. C. Pepeu, M. J. Kuhar, and S. J. Enna, eds.). Raven Press, New York, 107–116 (1980).
3. Yamamura, H. I., and S. H. Snyder. Muscarinic cholinergic receptor binding in longitudinal muscle of the guinea pig ileum with [^{3}H]quinuclidinyl benzilate. *Mol. Pharmacol.* **10**:861–867 (1974).
4. Aguilar, J. S., M. Criado, and E. DeRobertis. Protection by atropine of the inhibition caused by Triton X-100 on central muscarinic receptors. *Eur. J. Pharmacol.* **63**:251–257 (1980).
5. Fields, J. Z., W. R. Roeske, E. Morkin, and H. I. Yamamura. Cardiac muscarinic cholinergic receptors: biochemical identification and characterization. *J. Biol. Chem.* **253**:3251–3258 (1978).
6. Cuatrecasas, P., and M. Hollenberg. Membrane receptors and hormone action. *Adv. Protein Chem.* **30**:251–451 (1976).
7. Bürgisser, E., A. A. Hancock, R. J. Lefkowitz, and A. De Lean. Anomalous equilibrium binding properties of high-affinity racemic radioligands. *Mol. Pharmacol.* **19**:205–216 (1981).
8. De Robertis, E., M. Alberici, G. Rodríguez de Lores Arnaiz, and J. M. Azcurra. Isolation of different types of synaptic membranes from the brain cortex. *Life Sci.* **5**:577–582 (1966).
9. Lowry, O. H., N. J. Rosebrough, A. L. Farr, and R. J. Randall. Protein measurement with the Folin phenol reagent. *J. Biol. Chem.* **193**:265–275 (1951).
10. Bray, G. A. An efficient liquid scintillator for counting aqueous solutions. *Anal. Biochem.* **1**:274–278 (1960).
11. Marquardt, D. W. An algorithm for least-squares estimation of nonlinear parameters. *J. Soc. Indust. Appl. Math.* **11**:431–441 (1963).
12. Olsen, R. W., M. O. Bergman, P. C. Van Ness, S. C. Lummis, A. E. Watkins, C. Napias, and D. V. Greenlee. γ-aminobutyric acid receptor binding in mammalian brain: heterogeneity of binding sites. *Mol. Pharmacol.* **19**:217–227 (1981).
13. Thakur, A. K., L. J. Mitchell, and D. Rodbard. Graphical analysis of ligand-binding systems: evaluation by Monte Carlo studies. *Anal. Biochem.* **107**:279–295 (1980).
14. Bylund, D. B. Analysis of receptor binding data, in *Receptor Binding Techniques*. Society for Neuroscience, Cinncinnati, Ohio, 70–99 (1980).
15. Freeman, H. *Introduction to Statistical Inference*. Addison-Wesley Publishing Company, Reading, Mass. (1963).
16. Burgemeister, W., W. L. Klein, M. Nirenberg, and B. Witkop. Comparative binding studies with cholinergic ligands and histrionicotoxin at muscarinic receptors of neural cell lines. *Mol. Pharmacol.* **14**:751–767 (1978).
17. Hammer, R., C. P. Berrie, N. J. M. Birdsall, A. S. V. Burgen, and E. C. Hulme. Pirenzepine distinguishes between different subclasses of muscarinic receptors. *Nature* (*Lond.*) **283**:90–92 (1980).
18. Fisher, A., Y. Grunfeld, M. Weinstock, S. Gitter, and S. Cohen. A study of muscarinic receptor heterogeneity with weak antagonists. *Eur. J. Pharmacol.* **38**:131–139 (1976).
19. Fisher, A., M. Weinstock, S. Gitter, and S. Cohen. A new probe for heterogeneity in muscarinic receptors: 2-methyl-spiro(1,3-dioxolane-3,4)-quinuclidine. *Eur. J. Pharmacol.* **37**:329–338 (1976).